EVOLUTION IN THE PATTERNING OF ADIABATIC SHEAR BANDS

M. A. Meyers, Q. Xue, and V. F. Nesterenko
Department of Mechanical and Aerospace Engineering
University of California, San Diego, La Jolla, CA 92093

Abstract. The evolution of multiple adiabatic shear bands was investigated in stainless steel (different grain sizes: 30 and 140 μm), titanium, and Ti-6Al-4V alloy through the radial collapse of a thick-walled cylinder under high-strain-rate deformation (~10^4 s^{-1}) and different global strains(up to 0.9). Ti and Ti-6Al-4V displayed drastically different patterns of shear bands. The shear-band spacing is compared with one-dimensional theoretical predictions based on perturbation (Ockendon-Wright and Molinari) and momentum diffusion (Grady-Kipp) concepts. The experimentally observed spacing reveals a two-dimensional character of self-organization, not incorporated into the existing theories. A novel analytical description is proposed, in which embryos(potential initiation sites) are activated as a function of strain (greater than a threshold) according to a Weibull-type distribution. The model incorporates embryo disactivation by stress shielding as well as selective growth of shear bands. The imposed strain rate, embryo distribution, and rates of initiation and propagation determine the evolution of patterning.

INTRODUCTION

Shear bands have been the object of intense research in the past fifty years, since the classic work of Zener and Hollomon [1]. However, most of the studies focused on a single band and assumed a one-dimensional configuration. Notable exceptions are the experimental contributions of Bowden [2] in polymers and Shockey and Erlich [3]in steels and the analyses developed by Grady [4], Wright and Ockendon [5], Grady and Kipp [6], and Molinari [7]. This paper describes results of an effort aimed at understanding the evolution of shear-band spacing.

EXPERIMENTAL PROCEDURE

The experimental procedure consisted of subjecting thick-walled cylinders to controlled collapse by means of explosives placed on the periphery, in a cylindrical geometry with initiation at one of the extremities. The procedure is described in detail by Nesterenko and Bondar [8] and Nesterenko et al. [9]. Only the principal features are presented here. The collapse of thick-walled cylinder specimen is controlled by selected dimensions of copper tubes sandwiched in the sample. The strain rate imparted is on the order of $10^4 s^{-1}$. The collapse of the cylinder generates the highest shear strains along the internal surface. The unstable deformation, which is initially homogeneous, gives rise to shear bands along the internal surface. These bands grow inward to the thick-walled cylinder. They follow a spiral trajectory. The effective strain is defined by:

$$\varepsilon_{ef} = \frac{2}{\sqrt{3}} \varepsilon_{rr} = \frac{2}{\sqrt{3}} \ln\left(\frac{r_0}{r_f}\right), \qquad (1)$$

where r_0, r_f are the initial and final radii. Three materials, stainless steel 304L, CP titanium, and Ti-6Al-4V, were used. The shear band spacing, L_i, and length, l_i, the edge displacements, δ_i, were measured at different global strains.

MEASURED AND PREDICTED SPACINGS

Grady [4] was the first to propose a perturbation solution to shear instability of brittle materials. Wright and Ockendon [5] also developed a theoretical model, based on small perturbations. The predicted spacing is expressed as:

$$L_{WO} = 2\pi\left(\frac{m^3 kC}{\dot{\gamma}_0^3 a^2 \tau_0}\right)^{1/4}, \qquad (2)$$

where a is the thermal softening coefficient; k is the thermal conductivity; C is the heat capacity; τ_0 is the shear flow stress. m is the strain rate sensitivity. Grady and Kipp [6] extended Mott's [10] analysis for dynamic fracture to deformation localization. Momentum diffusion was considered as the dominant mechanism of shear bands. The spacing is:

$$L_{GK} = 2\left[\frac{9kC}{\dot{\gamma}_0^3 a^2 \tau_0}\right]^{1/4}. \quad (3)$$

Molinari [7] modified the WO model by introducing strain hardening effect:

$$L_{M'} = 2\pi\left[1-\frac{3}{4}\frac{\rho c}{\beta\tau_0^2}\frac{n(1-aT)}{\beta a\gamma}\right]^{-1}\cdot\left[\frac{kCm^3(1-aT_0)^2}{(1+m)\dot{\gamma}_0^3 a^2\tau_0}\right]^{1/4}, \quad (4)$$

where n is the strain hardening index.

The measured spectra of shear bands in 304SS, CP titanium and Ti-6Al-4V alloy are shown in Figure 1 at two global effective strains: 0.55 and 0.92 (for 304SS and CP Ti, Figs 1(a)-(f)); 0.13 and 0.26 (for Ti-6Al-4V, Fig. 1(g,h)). The numbers of shear bands at both the early and later stages are similar in SS 304 and Ti. There is no significant effect of grain size on shear band patterning for 304SS from Figs. 1(a)-(d).

Table 1 shows the comparison of experimental and predicted results. The grain size has only a minor effect on the spacing for 304SS, in the range investigated. The predicted results from Grady-Kipp model are roughly 20 times larger than measured values for Ti and 304SS, and twice for Ti-6Al-4V. On the other hand, the WO and M models provide reasonable estimates for Ti and 304SS but not for Ti-6Al-4V. The new data for Ti spacing presented here is different from the reported one [9,11] because detailed microstructural examination shows more fine pattern of bands nucleated along the internal boundary of the cylindrical specimens; the previous result only provided a count of well-developed bands. The failure of these theoretical predictions for Ti-6Al-4V alloy suggests that some mechanisms of shear band development have not been included into the above theories. One very important factor that is not incorporated into these theories is the two-dimensional nature of interactions among growing bands, which increases with their size. This was recognized by Nemat Nasser et al. [12] for parallel propagating cracks. A conceptually similar analysis is presented in the next section.

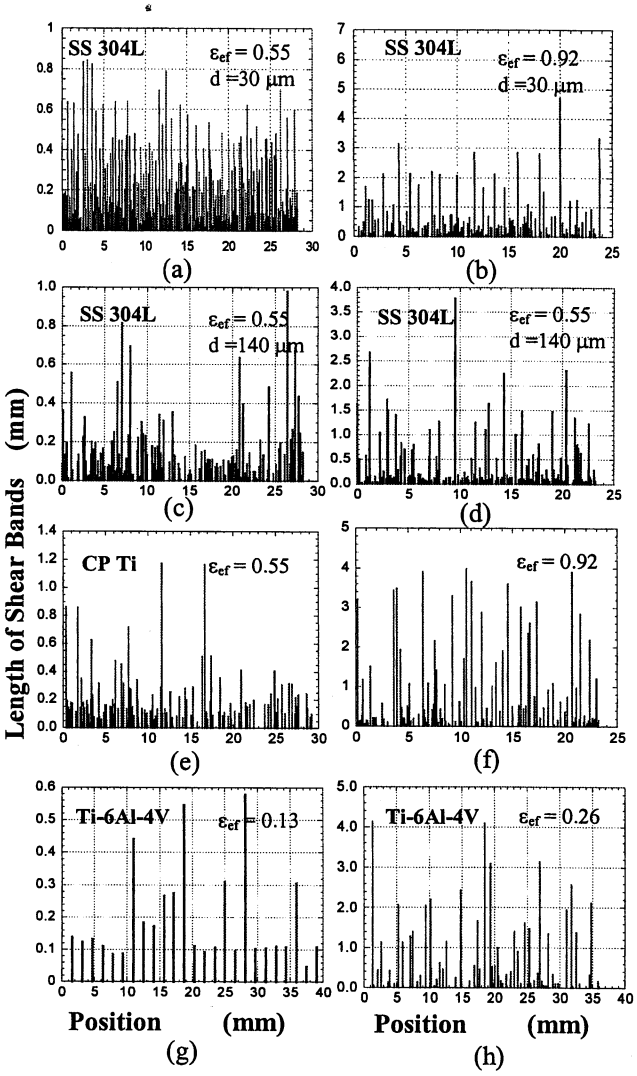

Figure 1. Configuration of shear-band lengths and spacings at different imposed strains for (a, b) AISI 304 SS, d=30 μm ; (c, d) AISI 304 SS, d=140 μm; (e, f) CP titanium; (g, h) Ti-6Al-4V alloy

TWO-DIMENSIONAL MODEL FOR SHEAR BAND SPACING

The failure of the one-dimensional models to explain the evolution of shear–band spacing led to proposed model below.

Initiation of shear bands is assumed to require a critical strain. Heterogeneous microstructural or surface effects (boundary geometry, defects orientation of grains, etc.) determine the range of strains in which the nucleation takes place. A heterogeneous nucleation process which is characterized as the selective activation of sites will

Table 1 Predictions and Experimental Spacings For 304SS Ti, and Ti-6%Al-4%V

Spacing(mm)	Exp. Data Initial level	L_{WO}(mm)	L_{GK}(mm)	L_{MO} (mm) (Without strain hardening)	L_{MO} (mm) (with strain hardening)
SS 304L	0.12	0.33	2.40	0.29	--
CP Titanium	0.18	0.29	2.13	0.24	0.64
Ti-6Al-4V	0.53	0.1	1.15	0.09	0.10

be assumed.

The probability of nucleation is given by $P(V_0,S_0)$, in a reference volume, V_0, or surface, S_0, depending on whether initiation occurs in the bulk or on the surface. It can be described by a modified Weibull distribution, using strain as the independent variable:

$$P(V_0, S_0) = 1 - \exp\left[-\left(\frac{\varepsilon - \varepsilon_i}{\varepsilon_0 - \varepsilon_i}\right)^q\right], \quad (5)$$

where ε_i is the critical strain below which no initiation takes place; ε_0 is the average nucleation strain (material constant); ε is the variable; and q is a Weibull modulus. For different materials the nucleation curve can have different shapes and positions, adjusted by setting q, ε_i, and ε_0. For Ti and Ti-6Al-4V, the mean nucleation strains are selected as 0.4 and 0.12, respectively, to best fit the experimental results; q was given values of 2, 3, 6, and 9, providing different distributions. Figures 2 (a) and (b) show the predicted distributions of initiation strains for Ti and Ti-6Al-4V, respectively.

There is a continuing shielding effect so that the bands that actually grow can be a fraction of the total possible initiation sites. Figure 3 shows the schematic interaction among embryos with growing strains (increasing time). As the result of unloading

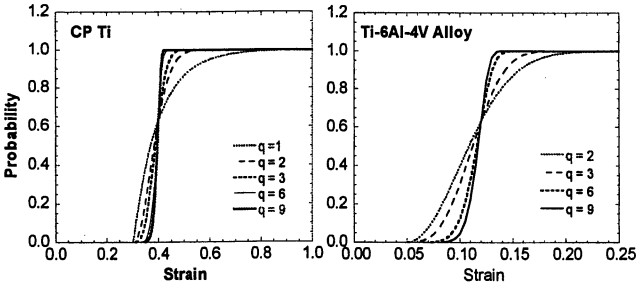

Figure 2. Probability of nucleation as a function of strain for (a) CP titanium; (b) Ti-6Al-4V alloy.

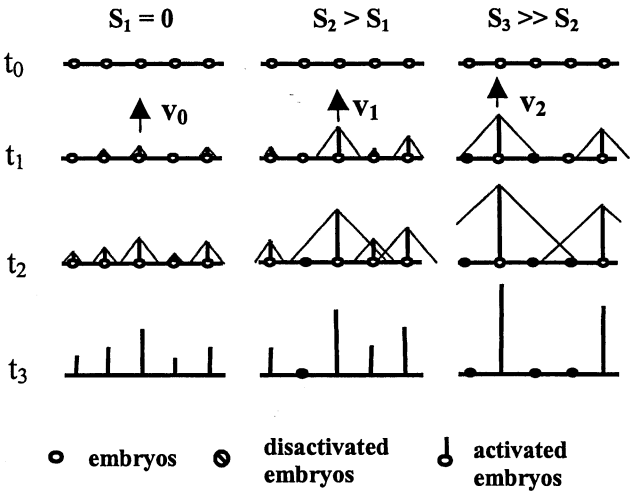

Figure 3. Two-dimensional representation of concurrent nucleation and shielding.

due to thermal softening inside bands, each growing band generates a shielded region around itself. Three factors govern the evolution of self-organization: (a) the strain rate, $\dot{\varepsilon}$; (b) the velocity of growth of shear band, V; (c) the initial spacing, l. Different scenarios emerge, depending on the growth velocity V. The activation of embryos at three times, t_1, t_2, and t_3, is shown in Figure 3. When V is low, the embryos are all activated before shielding can occur, and the natural spacing L_0 establishes itself. As V increases, shielding becomes more and more important, and the number of disactivated embryos increases. The shielded volume is dependent on the velocity of propagation of stress unloading and is given by k_1V, where $k_1<1$. The width of the unloaded region is $2k_1$ times the length of the shear band. The shielding effect can be expressed by S:

$$S = 1 - \frac{\dot{\varepsilon}L}{k_0 k_1 V} \quad (6)$$

The parameter k_0 defines the range of strains over which nucleation occurs. It can be set as $k_0 = 2(\varepsilon_0-\varepsilon_i)$. This expression correctly predicts an increase in shielding S with increasing V, decreasing $\dot{\varepsilon}$, and decreasing L. For an extremely large velocity of propagation of shear band, the critical time is very small and the shielding factor is close to one, which means almost complete shielding. The probability of nucleation under shear band shielding, $P(L)$, is obtained by adding Eqn. 6 into Eqn. 5:

$$P(L) = (1-S)P(V_0, S_0), \tag{8}$$

$$P(L) = \begin{cases} \left(\dfrac{\dot{\varepsilon}L}{2(\varepsilon_0-\varepsilon_i)V}\right)\left\{1-\exp\left[-\left(\dfrac{\varepsilon-\varepsilon_i}{\varepsilon_0-\varepsilon_i}\right)^q\right]\right\} & \text{if} \quad t_{cr} < \bar{t} \\ \left\{1-\exp\left[-\left(\dfrac{\varepsilon-\varepsilon_i}{\varepsilon_0-\varepsilon_i}\right)^q\right]\right\} & \text{if} \quad t_{cr} \geq \bar{t} \end{cases} \tag{9}$$

When $S = 0$ no shielding effect exists and all nuclei grow. If, in other extreme case, $S = 1$, no nucleation can happen. Figure 4(a) shows predicted evolutions of nucleation probabilities as a function of increasing strain, for different values of the shielding factor, S: 0, 0.2, 0.4, 0.6. This simple model shows how the initial distribution of activated embryos can be affected by different parameters. Xue et al. [13] present a more complete version of this analysis. It explains, qualitatively, the smaller spacing of shear bands in Ti, as compared to Ti-6Al-4V.

The shear-band spacing, corrected for shielding, is represented by:

$$L_S = \frac{L_{WO}}{P(L)\big|_{t>\bar{t}}} = \frac{L_{WO}}{(1-S)}. \tag{10}$$

L_{WO} is the Wright-Ockendon spacing. This spacing is plotted as a function of plastic strain, at a fixed value of S, in Figure 4(b). It is clear that the shear-band spacing decreases with strain until a final, steady state value is reached (Fig.4(b)). Using the calculated shielding factors S of 0.14 for Ti and 0. 89 for Ti-6Al-4V, the corresponding values for L_S are 0.34 and 0.9 mm, respectively. These values only approximate the experimental results (0.18 and 0.53 mm, respectively) but they have the correct trend. The agreement is satisfactory. During growth, an analogous selection process takes place, leading to a discontinuous increase in the spacing of the shear bands as their length increases, as described by Xue et al. [13,14].

ACNOWLEDGMENTS

Work supported by U.S. Army Research Office MURI Program No. DAAH004-96-1-0376.

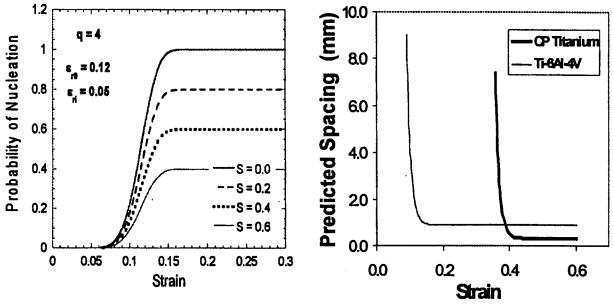

(a) (b)

Figure 4. Probability of nucleation incorporating shielding factor; (a) schematic; (b) probabilities and respective shear-band spacing for titanium and Ti-6Al-4V alloy

REFERENCES

1. Zener C. and Hollomon J. H., *J. Appl. Phys.*, **15,** 22 (1944)
2. Bowden, P. B., *Phil. Mag.*, **22,** 455-462 (1970).
3. Shockey D.A. and Erlich D.C., In *Shock Waves and High-Strain-Rate Phenomena in Metals* (eds. Meyers, M.A. and Murr, L. E.), Plenum Press, New York, (1981) pp. 249-261.
4. Grady, D. E., *J. Geophys. Res.*, **85,** 913-924(1980).
5. Wright, T.W., and Ockendon, H., *Int. Journal of Plasticity*, **12,** 927-34 (1996).
6. Grady, D.E., and Kipp, M.E., *J. Mech. Phys. Solids,* **35,** 95-118 (1987).
7. Molinari, A., *J. Mech. Phys. Sol.* **45,** 1551-75(1997).
8. Nesterenko, V.F., Bondar, M.P., *DYMAT Journal*, **1,** 245- (1994).
9. Nesterenko, V.F., Meyers, M.A., and Wright, T.W., *Acta Mat.*, **46,** 327-340 (1998).
10. Mott,N. F., *Proc. Roy. Soc.*,**189,** 300 (1947)
11. Xue, Q., Nesterenko, V. F, and M. A., Meyers, in CP505, *Shock Compression of Condensed Matter-1999* (eds. M.D. Furnish et al.), AIP, New York, (1999) pp. 431- 434.
12. Nemat Nasser, S., Keer, L. M., and Parihar, K. S., *J. Sol. Struct.*, **14,** 409(1978).
13. Xue, Q., Meyers, M. A., and Nesterenko, V. F., *Acta Mat.*, submitted(2001).
14. Nesterenko,V. F., Xue, Q., and Meyers, M. A., *J. Phys.*IV, **10,** 9-269-9-274(2000).